

Chemical pressure manipulation of ferromagnetism in magnetic semiconductor $Ba(Zn,Mn,Cu)_2As_2$

Xueqin Zhao(赵雪芹), Jinou Dong(董金瓯), Lingfeng Xie(谢玲凤), Xun Pan(潘洵), Haoyuan Tang(唐浩原), Zhicheng Xu(徐之程), and Fanlong Ning(宁凡龙)

Citation: Chin. Phys. B, 2025, 34 (**10**): 107510. DOI: 10.1088/1674-1056/addbce
http://cpb.iphy.ac.cn; http://iopscience.iop.org/cpb

What follows is a list of articles you may be interested in

Unconventional room-temperature negative magnetoresistance effect in Au/n-Ge:Sb/Au devices

Xiong He(何雄), Fan-Li Yang(杨凡黎), Hao-Yu Niu(牛浩峪), Li-Feng Wang(王立峰), Li-Zhi Yi(易立志),Yun-Li Xu(许云丽), Min Liu(刘敏), Li-Qing Pan(潘礼庆), and Zheng-Cai Xia(夏正才)

Chin. Phys. B, 2024, 33 (**3**): 037504. DOI: 10.1088/1674-1056/ad15f8

Discovery of new potential magnetic semiconductors in quaternary Heusler compounds by addition of lanthanides

Jin Guo(郭金), Shiyi Feng(冯时怡), Rong Tao(陶容), Guoxia Wang(王国霞), Yue Wang(王越), and Zhifeng Liu(刘志锋)

Chin. Phys. B, 2023, 32 (**12**): 127509. DOI: 10.1088/1674-1056/acfaf7

Li_2NiSe_2: A new-type intrinsic two-dimensional ferromagnetic semiconductor above 200 K

Li-Man Xiao(肖丽蔓), Huan-Cheng Yang(杨焕成), and Zhong-Yi Lu(卢仲毅)

Chin. Phys. B, 2023, 32 (**3**): 037501. DOI: 10.1088/1674-1056/aca39f

Gd impurity effect on the magnetic and electronic properties of hexagonal Sr ferrites: A case study by DFT

Masomeh Taghipour, Mohammad Yousefi, Reza Fazaeli, Masoud Darvishganji

Chin. Phys. B, 2020, 29 (**7**): 077505. DOI: 10.1088/1674-1056/ab8d9f

Progress of novel diluted ferromagnetic semiconductors with decoupled spin and charge doping: Counterparts of Fe-based superconductors

Shengli Guo(郭胜利), Fanlong Ning(宁凡龙)

Chin. Phys. B, 2018, 27 (**9**): 097502. DOI: 10.1088/1674-1056/27/9/097502

Chemical pressure manipulation of ferromagnetism in magnetic semiconductor $Ba(Zn,Mn,Cu)_2As_2$

Xueqin Zhao(赵雪芹)[1], Jinou Dong(董金瓯)[1], Lingfeng Xie(谢玲凤)[1], Xun Pan(潘洵)[1], Haoyuan Tang(唐浩原)[1], Zhicheng Xu(徐之程)[1], and Fanlong Ning(宁凡龙)[1,2,3,4,†]

[1] *School of Physics, Zhejiang University, Hangzhou* 310027, *China*
[2] *Institute for Advanced Study in Physics, Zhejiang University, Hangzhou* 310027, *China*
[3] *State Key Laboratory of Silicon and Advanced Semiconductor Materials, Zhejiang University, Hangzhou* 310027, *China*
[4] *Collaborative Innovation Center of Advanced Microstructures, Nanjing University, Nanjing* 210093, *China*

(Received 30 April 2025; revised manuscript received 14 May 2025; accepted manuscript online 22 May 2025)

We report the manipulation of ferromagnetism in magnetic semiconductor $Ba(Zn,Mn,Cu)_2As_2$ through chemical pressure. The substitutions of Sr for Ba and Sb for As introduce positive and negative chemical pressures, respectively; neither Sr doping nor Sb doping change the tetragonal crystal structure. Based on $Ba(Zn_{0.75}Mn_{0.125}Cu_{0.125})_2As_2$ with $T_C \sim 34$ K, 10% Sr/Ba substitutions significantly improve T_C by $\sim 15\%$ to 39 K, whereas 10% Sb/As substitutions substantially reduce T_C by $\sim 47\%$ to 18 K. The AC magnetic susceptibility measurements indicate that Sr-doped and Sb-doped samples evolve into a spin glass state below the spin freezing temperature T_f. Electrical transport measurements demonstrate that Sr-doped specimens retain semiconducting behavior; additionally, they display a significant negative magnetoresistance effect under applied magnetic fields and the magnetoresistance reaches $\sim -19\%$ at 8 T.

Keywords: magnetic semiconductors, spin-glass, negative magnetoresistance

PACS: 75.50.Pp, 75.50.Lk, 75.30.Cr

DOI: 10.1088/1674-1056/addbce **CSTR:** 32038.14.CPB.addbce

1. Introduction

As an important branch in the field of spintronics research, magnetic semiconductors (MSs), which exhibits both characteristics of semiconductors and ferromagnets, have attracted extensive attentions.[1–5] The most representative MSs are the III–V MS (Ga,Mn)As thin films prepared through the low-temperature molecular beam epitaxy (LT-MBE) method.[6,7] When Mn doping level reaches $\sim 12\%$, the Curie temperature (T_C) is up to ~ 200 K.[8] Some spintronic devices based on (Ga,Mn)As have been fabricated.[5,9,10] However, in (Ga,Mn)As, Mn/Ga substitutions introduce both spins and carriers simultaneously, which hinders the independent manipulation of spins' and carriers' concentrations, thereby preventing us from investigating their individual contributions to the formation of ferromagnetic ordering.

Recently, many series of bulk MSs which are isostructure to the Fe-based superconductors have been reported, such as 111-type Li(Zn,Mn)As[11] and Li(Zn,Mn)P,[12] 122-type $(Ba,K)(Zn,Mn)_2As_2$[13] and $Ba(Zn,Mn,Cu)_2As_2$,[14] and 1111-type (La,Ba)(Zn,Mn)AsO[15] and (La,Ca)(Zn,Mn)SbO.[16] In these bulk MSs, spins and carriers are introduced independently, which enable us to separately control them. In addition, bulk form materials make it possible to the characterization of their microscopic magnetic properties by using experimental techniques such as muon spin resonance (μSR), nuclear magnetic resonance (NMR) and neutron scattering.[11,13,15,17,18] Among them, the bulk MS with the highest T_C observed experimentally is $(Ba,K)(Zn,Mn)_2As_2$ whose T_C reaches ~ 260 K.[19] Nevertheless, achieving room temperature ferromagnetic ordering in MSs remains a key scientific challenge.

For the purpose of improving the ferromagnetic transition temperature, in recent years, physical pressure and chemical pressure have been applied in manipulating the ferromagnetism of MSs.[20–26] For instance, applying a hydrostatic pressure of 2.7 GPa to the III–V MS (In,Mn)Sb, T_C has increased by $\sim 25\%$;[20] both physical pressure and chemical pressure have suppressed the T_C of $(Ba,K)(Zn,Mn)_2As_2$;[22–24] in (La,Ca)(Zn,Mn)AsO, Y/La substitutions introduce positive chemical pressure and 7.5% Y doping which is equivalent to applying physical pressure of 0.521 GPa has improved T_C by $\sim 30\%$.[26] $Ba(Zn,Mn,Cu)_2As_2$, the first MS with Mn and Cu co-doped at the Zn sites to introduce spins and carriers, respectively, shares the same crystal structure with the Fe-based superconductor $(Ba,K)Fe_2As_2$[27] and the antiferromagnet $BaMn_2As_2$,[28] which would be promising to fabricate potential heterostructure devices. However, the effect of chemical pressure on the ferromagnetic transition temperature in $Ba(Zn,Mn,Cu)_2As_2$ has not been investigated.

In this paper, we report the chemical pressure effect on the ferromagnetism in $Ba(Zn_{0.75}Mn_{0.125}Cu_{0.125})_2As_2$ which has a

†Corresponding author. E-mail: ningfl@zju.edu.cn

© 2025 Chinese Physical Society and IOP Publishing Ltd. All rights, including for text and data mining, AI training, and similar technologies, are reserved.

$T_C \sim 34$ K. Positive and negative chemical pressures are introduced by doping Sr into Ba sites to compress the lattice and doping Sb into As sites to expand the lattice, respectively. The x-ray diffraction measurements show that both Sr-doped and Sb-doped samples conserve the tetragonal crystal structure. We find that 10% Sr doping drastically improves T_C by $\sim 15\%$ to 39 K and 10% Sb doping significantly suppresses T_C by $\sim 47\%$ to 18 K. The AC magnetic susceptibility measurements demonstrate that Sr-doped and Sb-doped samples exhibit the characteristics of spin glass state below spin freezing temperature T_f. The resistivity measurements indicate that Sr-doped samples still retain semiconducting behavior; furthermore, Sr-doped samples exhibit an obvious negative magnetoresistance effect under applied external magnetic fields.

2. Experiments

Polycrystalline samples of Sr-doped $(Ba_{1-x}Sr_x)(Zn_{0.75}Mn_{0.125}Cu_{0.125})_2As_2$ ($x = 0$, 0.05, 0.10) and Sb-doped $Ba(Zn_{0.75}Mn_{0.125}Cu_{0.125})_2(As_{1-y}Sb_y)_2$ ($y = 0$, 0.05, 0.10) were prepared via the solid-state reaction method. First of all, high-purity Zn, Mn, Cu, As, Sb were mixed according to the nominal composition and were placed in the aluminum crucibles, then sealed in evacuated silica tubes. The mixtures were heated to 500 °C and 800 °C, and kept for 10 h and 20 h, respectively, to make the precursors $(Zn_{0.75}Mn_{0.125}Cu_{0.125})As$ and $(Zn_{0.75}Mn_{0.125}Cu_{0.125})(As_{1-y}Sb_y)$. Next, the mixtures of Ba, Sr, and $(Zn_{0.75}Mn_{0.125}Cu_{0.125})As$ or $(Zn_{0.75}Mn_{0.125}Cu_{0.125})(As_{1-y}Sb_y)$ were placed in the aluminum crucibles, sealed in evacuated silica tubes, then heated to 750 °C, 900 °C, and 1100 °C, and kept for 10 h, 10 h, and 20 h, respectively. After that, the products were fully grounded, pressed into pellets, placed in alumina crucibles, sealed in evacuated silica tubes again and then reheated to 1000 °C for 25 h. All operations except the sealing of silica tubes were performed in a glove box filled with high-purity argon.

The crystal structure of polycrystalline samples was characterized by a powder x-ray diffractometer (Model EMPYREAN) with monochromatic Cu-$K_{\alpha 1}$ radiation. The detailed lattice parameters were determined through Rietveld refinements using open-source GSAS-II package.[29] The DC and AC magnetizations were performed on a Quantum Design magnetic property measurement system (MPMS-3). The electrical resistivity and magnetoresistance were measured on a Quantum Design physical property measurement system (PPMS).

3. Results and discussion

In Fig. 1(a), we show the x-ray diffraction patterns of Sr-doped $(Ba_{1-x}Sr_x)(Zn_{0.75}Mn_{0.125}Cu_{0.125})_2As_2$ ($x = 0$, 0.05, 0.10) and Sb-doped $Ba(Zn_{0.75}Mn_{0.125}Cu_{0.125})_2(As_{1-y}Sb_y)_2$ ($y = 0$, 0.05, 0.10). The Bragg peaks for all samples can be well indexed by the tetragonal structure with the $I4/mmm$ space group. That is to say, Sr/Ba or Sb/As substitutions do not change the crystal structure of $Ba(Zn,Mn,Cu)_2As_2$, as shown in the inset of Fig. 1(b), in which ZnAs layers (formed by $ZnAs_4$ tetrahedra) and Ba layers are alternately stacked along the c-axis. A few small peaks of ZnSb impurities as marked by the stars (*) in Fig. 1(a) have been observed in Sb-doped samples. These ZnSb impurities are non-magnetic, thus they will not affect the discussion of magnetism in the following. The lattice parameters were calculated by Rietveld refinements based on GSAS-II package.[29] In Fig. 1(b), we take the sample $(Ba_{0.90}Sr_{0.10})(Zn_{0.75}Mn_{0.125}Cu_{0.125})_2As_2$ as an example to present the result of Rietveld refinement, where the resultant weighted reliable factor R_{wp} is $\sim 6.3\%$, indicating that our samples are in good quality. In Figs. 1(c) and 1(d), we show the lattice constants a and c, as well as the Zn(Mn)–As(Sb) bond length d and the As(Sb)–Zn(Mn)–As(Sb) bond angle α. Since the ionic radius of Sb^{3-} is larger than that of As^{3-}, for the Sb-doped samples, with the increasing of Sb doping level, the lattice constants a, c, and bond length d show an increasing trend, which confirms that the substitution of As by Sb introduces negative chemical pressure; in contrast, since the ionic radius of Sr^{2+} is smaller than that of Ba^{2+}, for the Sr-doped samples, as the Sr doping level increases, a, c, and d monotonically decrease, which verifies that the substitution of Ba by Sr does indeed introduce positive chemical pressure. Meanwhile, with the increasing of Sb doping level, the bond angle α decreases and gradually deviate from the ideal tetrahedral bond angle value of 109.47°; while with more Sr doping, the bond angle α increases and gradually approach 109.47°.

In Fig. 2(a), we show the temperature-dependent magnetization in zero-field-cooling (ZFC) and field-cooling (FC) modes under an applied field $H_{ext} = 100$ Oe (1 Oe = 79.5775 A·m^{-1}) for both Sr-doped and Sb-doped samples. As the temperature decreases, the magnetization of all samples exhibits a sudden increase, which demostrates the onset of ferromagnetic transition. At lower temperatures, the $M(T)$ curves split in ZFC and FC modes, and a cusp appears on the ZFC curve at a temperature defined as spin freezing temperature T_f. From the inset of Fig. 2(a), we can clearly see the evolution of ferromagnetic transition with the variation of Sr or Sb doping level. As the Sr doping level increases, the ferromagnetic transition temperature shifts towards the higher temperature region and the magnetization at 2 K, M_{base}, monotonously increases. On the other hand, with the increasing of Sb doping level, the ferromagnetic transition temperature quickly shifts towards the lower temperature region and M_{base} significantly reduces.

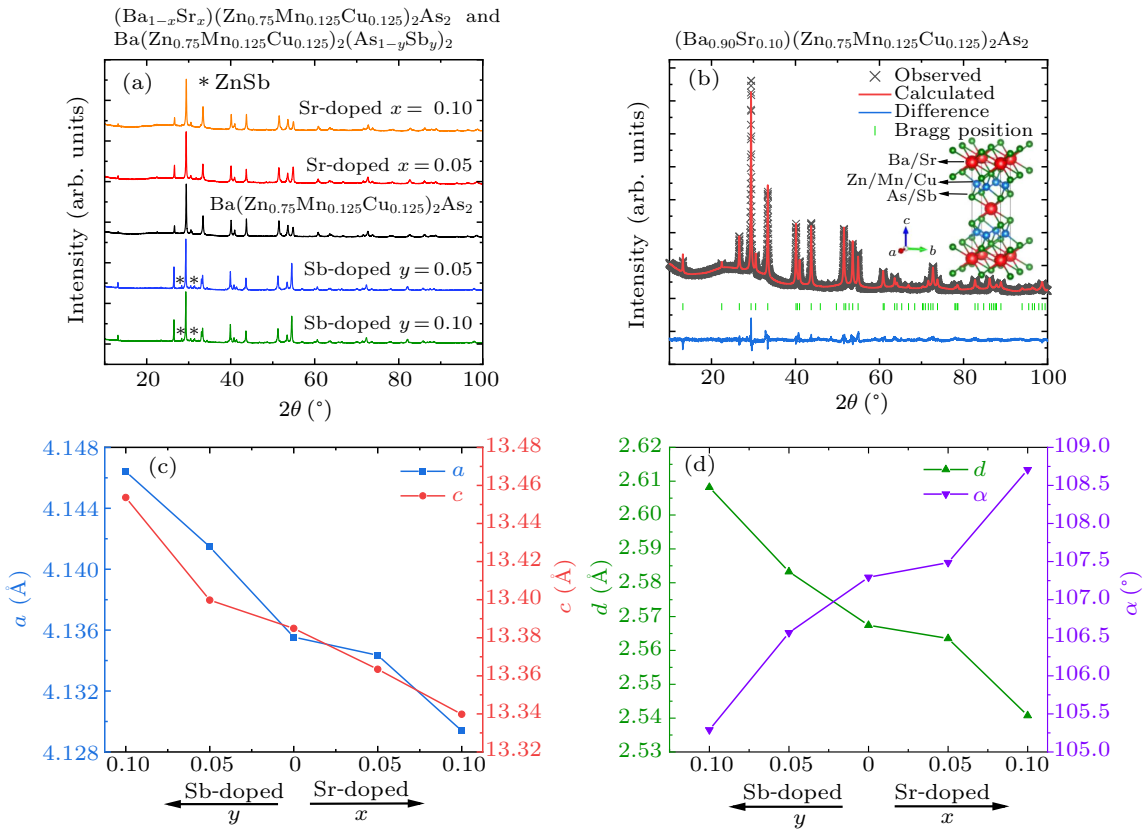


Fig. 1. (a) The x-ray diffraction patterns of Sr-doped $(Ba_{1-x}Sr_x)(Zn_{0.75}Mn_{0.125}Cu_{0.125})_2As_2$ (x = 0, 0.05, 0.10) and Sb-doped $Ba(Zn_{0.75}Mn_{0.125}Cu_{0.125})_2(As_{1-y}Sb_y)_2$ (y = 0, 0.05, 0.10). Traces of impurities ZnSb (*) are marked for Sb-doped samples. (b) The Rietveld refinement of $(Ba_{0.90}Sr_{0.10})(Zn_{0.75}Mn_{0.125}Cu_{0.125})_2As_2$. Inset shows the crystal structure of $BaZn_2As_2$. (c) The lattice constants a and c for both Sr-doped and Sb-doped samples. (d) The Zn(Mn)–As(Sb) bond length d and the As(Sb)–Zn(Mn)–As(Sb) bond angle α for both Sr-doped and Sb-doped samples.

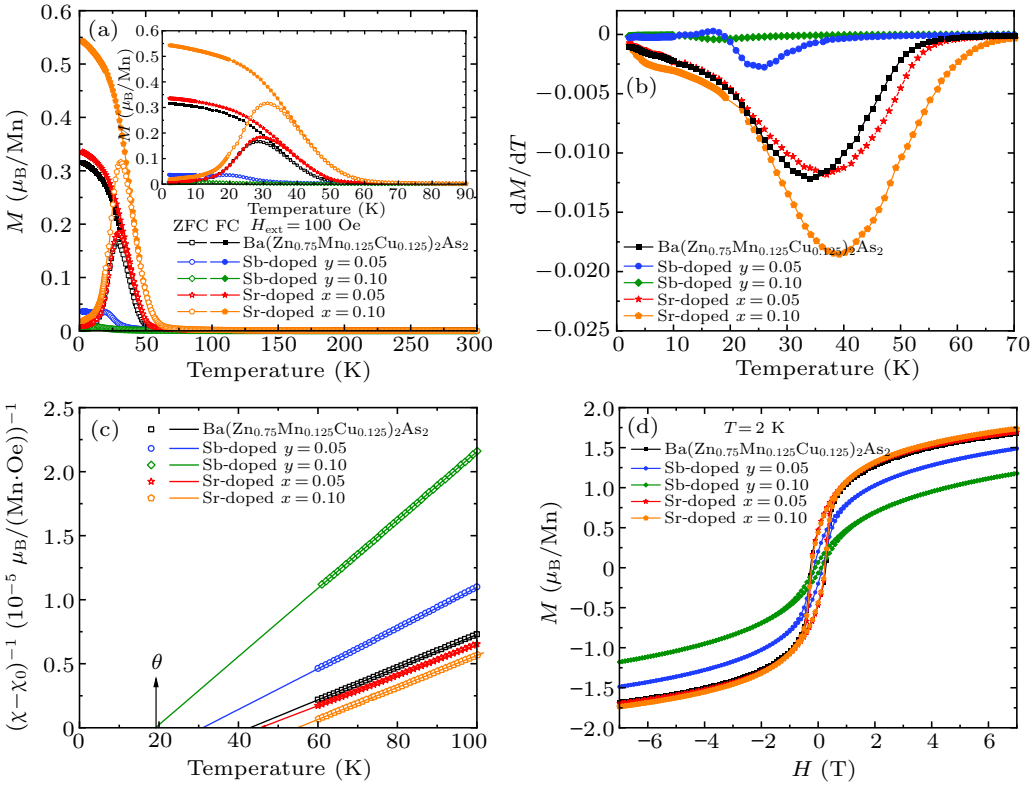


Fig. 2. (a) The temperature dependence of DC magnetization for Sr-doped and Sb-doped samples under zero-field-cooling (ZFC) and field-cooling (FC) modes in an external magnetic field H_{ext} = 100 Oe. Inset shows the enlarged $M(T)$ curves in the temperature range of 2 K–90 K for all samples. (b) The $dM(T)/dT$ versus T curves for Sr-doped and Sb-doped samples. (c) The plot of $1/(\chi-\chi_0)$ versus T for Sr-doped and Sb-doped samples. The straight lines represent the fitting of Curie–Weiss law. (d) The iso-thermal magnetization for both Sr-doped and Sb-doped samples measured at 2 K.

In order to visualize the change of ferromagnetic transition temperature T_C with Sr or Sb doping level, we plot the $dM(T)/dT$ versus T curves under FC mode in Fig. 2(b). The minimum value of $dM(T)/dT$ corresponds to T_C. Compared with the starting compound $Ba(Zn_{0.75}Mn_{0.125}Cu_{0.125})_2As_2$ which has a $T_C \sim 34$ K, with the increasing of Sr doping level, T_C monotonically improves and reaches 39 K when the Sr doping level x is 0.10; however, as the Sb doping level increases, T_C gradually decreases and is suppressed to 18 K with the Sb doping level $y = 0.10$. We fit the magnetic susceptibility data in high temperature region using the Curie–Weiss law $\chi = \chi_0 + C/(T-\theta)$, in which C is the Curie constant, χ_0 represents a temperature-independent term and θ is the Weiss temperature. The fitting results of $1/(\chi-\chi_0)$ versus T are plotted in Fig. 2(c), and we can obtain the Weiss temperature from the intersections of the fitting lines and x-axis. It can be seen that all θ are positive, further indicating the existence of ferromagnetic interaction in the systems. As the Sr doping level increases, θ shows an increasing trend, which is another sign of enhanced ferromagnetic interaction; while with more Sb doping, θ decreases gradually. In addition, using formula $C = N\mu_0\mu_{eff}^2/3k_B$, we can calculate the effective moment μ_{eff}, as shown in Table 1. In Fig. 2(d), we show the iso-thermal magnetization curves $M(H)$ measured at 2 K for the samples with different Sr or Sb doping level. The clear hysteresis loop confirms the existence of ferromagnetic interaction.

In Table 1, we tabulate the base temperature moment M_{base} (the magnetization measured at $T = 2$ K and $H_{ext} = 100$ Oe under FC mode), the Curie temperature T_C, the Weiss temperature θ, and the effective moment μ_{eff}. We can see that both T_C and θ increase with more Sr doping, while they gradually decrease with more Sb doping. That is, the introduction of positive chemical pressure through Sr/Ba substitutions is conducive to enhancing the ferromagnetic interaction and thereby improves the ferromagnetic transition temperature. The case of Sb doping is on the opposite, which is similar to the behavior observed in Sb-doped P-type MS $(Ba,K)(Zn,Mn)_2As_2$.[24] For bulk MS $(Ba,K)(Zn,Mn)_2As_2$, many theoretical and experimental results indicate that the ferromagnetic interaction between the local moments is mediated by the p states of As through As 4p-Mn 3d hybridization.[22,30] By investigating the effect of physical pressure effects on the ferromagnetism of $(Ba,K)(Zn,Mn)_2As_2$, Sun *et al.*[23] have found that the shortening of Zn(Mn)–As bond length d and the As–Zn(Mn)–As bond angle α closer to the ideal tetrahedral bond angle value of 109.47° will enhance the coupling strength between the As 4p and Mn 3d orbitals, which plays a key role in the formation of ferromagnetic interactions. That is, the geometric structure of the $Zn(Mn)As_4$ tetrahedron directly affects the p–d hybridization, thereby leading to the change of ferromagnetic interactions (T_C) in the systems. In current work, combined with the crystal structure parameters and magnetic measurement results, we find that when Sr/Ba substitution introduces positive chemical pressure into the system, the Zn(Mn)–As bond length is shortened and the As–Zn(Mn)–As bond angle gradually approaches 109.47°, which enhances T_C. These findings are parallel to the experimental observations on ferromagnetism regulation through chemical pressure effects in N-type MS $Ba(Zn,Co)_2As_2$.[25]

Table 1. The base temperature moment M_{base}, the Curie temperature T_C, the Weiss temperature θ, and the effective moment μ_{eff}.

Doping level	M_{base} (μ_B/Mn)	T_C (K)	θ (K)	μ_{eff} (μ_B/Mn)
Sb-doped 0.10	0.007	18	19	3.86
Sb-doped 0.05	0.036	26	31	5.03
$Ba(Zn_{0.75}Mn_{0.125}Cu_{0.125})_2As_2$	0.316	34	43	5.91
Sr-doped 0.05	0.335	37	46	6.12
Sr-doped 0.10	0.543	39	55	5.97

In the report on MS $Ba(Zn_{0.75}Mn_{0.125}Cu_{0.125})_2As_2$ in 2015, the AC susceptibility measurement results have shown that the T_f depends on the applied frequency f, which is a classic signature of spin glass.[14] For the purpose of determining whether the Sr-doped and Sb-doped samples exhibit the behavior of spin glass, we conducted the AC susceptibility at different frequencies f for both Sr-doped and Sb-doped samples. In Figs. 3(a)–3(d), we show the real part χ' of the AC susceptibility. As frequency f increases, the cusp positions of χ' for both Sr-doped and Sb-doped samples slightly shift towards the higher temperatures, which is a hallmark of spin glass system. In addition, the frequency dependence of T_f can be characterized by the equation $K = \Delta T_f/[T_f \Delta \log f]$.[31] Taking the sample $Ba(Zn_{0.75}Mn_{0.125}Cu_{0.125})_2(As_{0.95}Sb_{0.05})_2$ as an example, we obtained $K \sim 0.022$, which is within the range of spin glass system ($K \sim 0.005$–0.08).[32] These indicate that our samples evolve into a spin glass state below the spin freezing temperature T_f.

We performed the electrical transport measurements on Sr-doped samples. In Fig. 4(a), we perform temperature-dependent resistivity $\rho(T)$ at zero field. As the temperature decreases, the resistivity increases, indicating that the Sr-doped samples retain semiconducting behavior. Moreover, the

resistivity decreases with the increasing of Sr doping level. This is caused by the pressure effect leading to electronic bandwidth broadening and carrier mobility increasing.[22] In Fig. 4(b), we show the temperature-dependent magnetoresistance for $(Ba_{0.90}Sr_{0.10})(Zn_{0.75}Mn_{0.125}Cu_{0.125})_2As_2$ under different applied magnetic fields. With the increasing of magnetic field, the resistivity is suppressed rapidly, demonstrating a negative magnetoresistance phenomenon, which is due to the suppression of spin-dependent scattering under the external magnetic field. The negative magnetoresistance ($MR \equiv [\rho(H) - \rho(0)]/\rho(0)$) reaches $\sim -19\%$ at $T = 2$ K and $H_{ext} = 8$ T, as shown in the inset of Fig. 4(b).

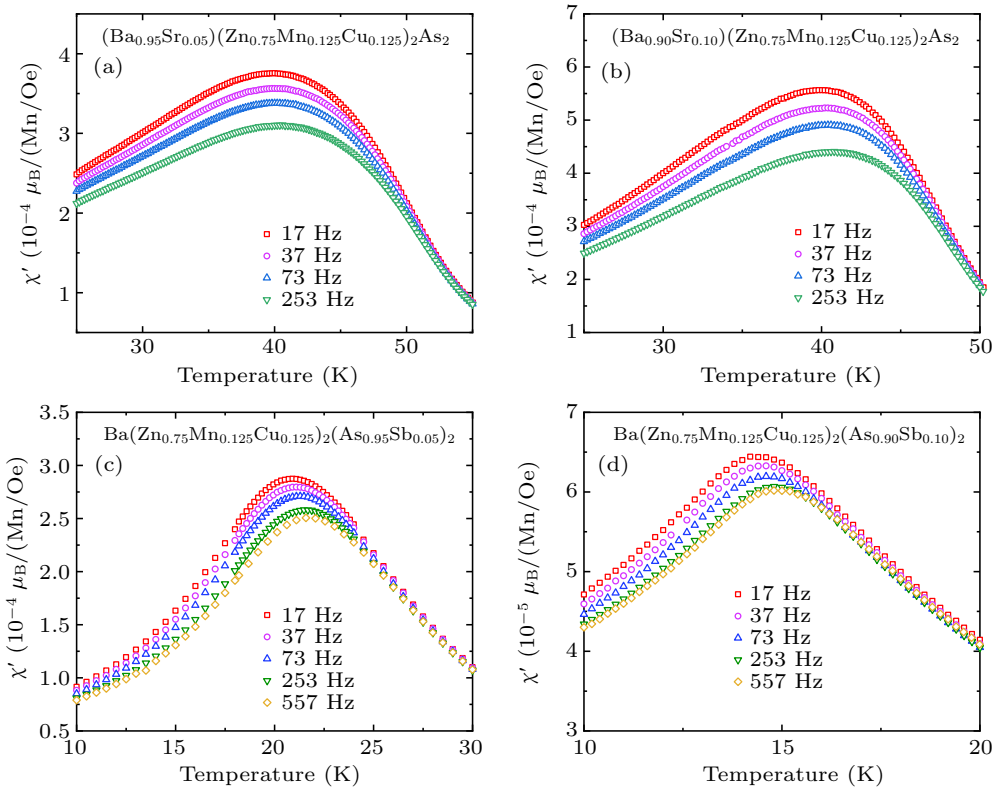


Fig. 3. The real part χ' of AC magnetic susceptibility for (a) $(Ba_{0.95}Sr_{0.05})(Zn_{0.75}Mn_{0.125}Cu_{0.125})_2As_2$, (b) $(Ba_{0.90}Sr_{0.10})(Zn_{0.75}Mn_{0.125}Cu_{0.125})_2As_2$, (c) $Ba(Zn_{0.75}Mn_{0.125}Cu_{0.125})_2(As_{0.95}Sb_{0.05})_2$, and (d) $Ba(Zn_{0.75}Mn_{0.125}Cu_{0.125})_2(As_{0.90}Sb_{0.10})_2$ at different frequencies f.

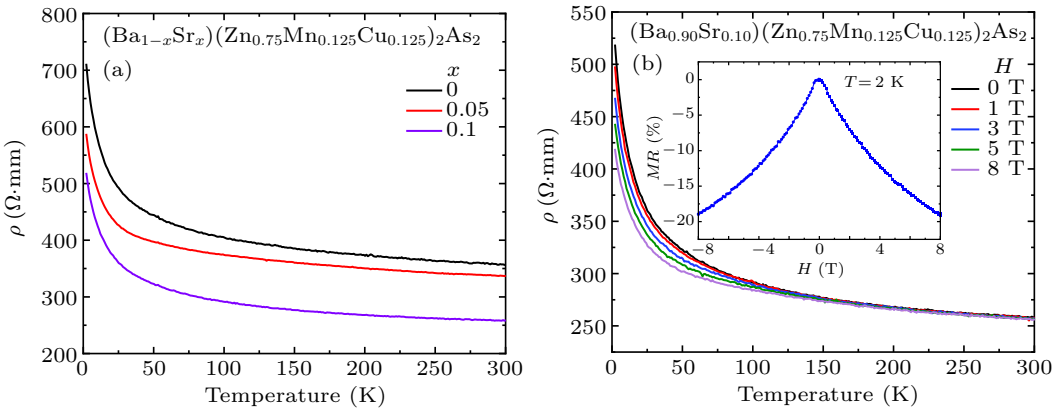


Fig. 4. (a) The temperature-dependent resistivity $\rho(T)$ for Sr-doped samples. (b) The temperature-dependent magnetoresistance for $(Ba_{0.90}Sr_{0.10})(Zn_{0.75}Mn_{0.125}Cu_{0.125})_2As_2$. The inset shows the field dependence of magnetoresistance MR measured in an external field ranging from 0 T to −8 T and 0 T to 8 T at 2 K.

4. Summary

To summerize, we have successfully synthesized both Sr-doped $(Ba_{1-x}Sr_x)(Zn_{0.75}Mn_{0.125}Cu_{0.125})_2As_2$ ($x = 0$, 0.05, 0.10) and Sb-doped $Ba(Zn_{0.75}Mn_{0.125}Cu_{0.125})_2(As_{1-y}Sb_y)_2$ ($y = 0$, 0.05, 0.10), in which equivalent Sr/Ba and Sb/As substitutions introduce positive and negative chemical pressures, respectively. The x-ray diffraction results indicate that both Sr-doped and Sb-doped samples retain the tetragonal crystal structure. Magnetization measurements show that T_C increases by $\sim 15\%$ to 39 K with 10% Sr doping and decreases by $\sim 47\%$ to 18 K with 10% Sb doping. On the other hand, the resistivity measurements reveal that the Sr-doped samples still

retain semiconducting behavior, that is, Sr doping improves the ferromagnetic transition temperature while conserving the high temperature tetragonal structure and the semiconducting behavior. Our work provides another experimental evidence that the geometric structure of $Zn(Mn)As_4$ tetrahedron plays a pivotal role in the ferromagnetism of 122-type $BaZn_2As_2$-based magnetic semiconductors; furthermore, the rational application of the pressure effect is beneficial to the development of novel magnetic semiconductors with higher ferromagnetic transition temperature.

Acknowledgements

Project supported by the National Key Research and Development Program of China (Grant Nos. 2022YFA1402701 and 2022YFA1403202), the National Natural Science Foundation of China (Grant No. 12074333), and the Key Research and Development Program of Zhejiang Province, China (Grant No. 2021C01002).

References

[1] Ohno H 1998 *Science* **281** 951
[2] Žutić I, Fabian J and Das Sarma S 2004 *Rev. Mod. Phys.* **76** 323
[3] Wolfand S A, Awschalom D D, Buhrman R A, Daughton J M, von Molnár S, Roukesand M L, Chtchelkanova A Y and Treger D M 2001 *Science* **294** 1488
[4] Dietl T 2010 *Nat. Mater.* **9** 965
[5] Dietl T and Ohno H 2014 *Rev. Mod. Phys.* **86** 187
[6] Munekata H, Ohno H and von Molnar S, Segmüller A, Chang L L and Esaki L 1989 *Phys. Rev. Lett.* **63** 1849
[7] Ohno H, Shen A, Matsukura F, Oiwa A, Endo A, Katsumoto S and Iye Y 1996 *Appl. Phys. Lett.* **63** 363
[8] Chen L, Yang X, Yang F H, Zhao J H, Misuraca J, Xiong P and von Molnár S 2011 *Nano Lett.* **11** 2584
[9] Ohno Y, Young D K, Beschoten B, Matsukura F, Ohno H and Awschalom D D 1999 *Nature* **402** 790
[10] Tanaka M 2020 *Jpn. J. Appl. Phys.* **60** 010101
[11] Deng Z, Jin C Q, Liu Q Q, Wang X C, Zhu J L, Feng S M, Chen L C, Yu R C, Arguello C, Goko T, Ning F L, Zhang J S, Wang Y Y, Aczel A A, Munsie T, Williams T J, Luke G M, Kakeshita T, Uchida S, Higemoto W, Ito T U, Gu B, Maekawa S, Morris G D and Uemura Y J 2011 *Nat. Commun.* **2** 422
[12] Deng Z, Zhao K, Gu B, Han W, Zhu J L, Wang X C, Li X, Liu Q Q, Yu R C, Goko T, Frandsen B, Liu L, Zhang J S, Wang Y Y, Ning F L, Maekawa S, Uemura Y J and Jin C Q 2013 *Phys. Rev. B* **88** 081203
[13] Zhao K, Deng Z, Wang X C, Han W, Zhu J L, Li X, Liu Q Q, Yu R C, Goko T, Frandsen B, Liu L, Ning F L, Uemura Y J, Dabkowska H, Luke G M, Luetkens H, Morenzoni E, Dunsiger S R, Senyshyn A, Böni P and Jin C Q 2013 *Nat. Commun.* **4** 1442
[14] Man H Y, Guo S L, Sui Y, Guo Y, Chen B, Wang H D, Ding C and Ning F L 2015 *Sci. Rep.* **5** 15507
[15] Ding C, Man H Y, Qin C, Lu J C, Sun Y L, Wang Q, Yu B Q, Feng C M, Goko T, Arguello C J, Liu L, Frandsen B A, Uemura Y J, Wang H D, Luetkens H., Morenzoni E, Han W, Jin C Q, Munsie T, Williams T J, D'Ortenzio R M, Medina T, Luke G M, Imai T and Ning F L 2013 *Phys. Rev. B* **88** 041102
[16] Han W, Zhao K, Wang X C, Liu Q Q, Ning F L, Deng Z, Liu Y, Zhu J L, Ding C, Man H Y and Jin C Q 2013 *Sci. China- Phys. Mech. Astron.* **56** 2026
[17] Ding C, Qin C, Man H Y, Imai T and Ning F L 2013 *Phys. Rev. B* **88** 041108
[18] Ning F L, Man H Y, Gong X, Zhi G X, Guo S L, Ding C, Wang Q, Goko T, Liu L, Frandsen B A, Uemura Y J, Luetkens H, Morenzoni E, Jin C Q, Munsie T, Luke G M, Wang H D and Chen B 2014 *Phys. Rev. B* **90** 085123
[19] Peng Y, Li X, Shi L C, Zhao G Q, Zhang J, Zhao J F, Wang X C, Gu B, Deng Z, Uemura Y J and Jin C Q 2025 *Adv. Phys. Res.* **4** 2400124
[20] Csontos M, Mihaly G, Jankó B, Wojtowicz T, Liu X and Furdyna J K 2005 *Nat. Mater.* **4** 447
[21] Gryglas-Borysiewicz M, Kwiatkowski A, Baj M, Wasik D, Przybytek J and Sadowski J 2010 *Phys. Rev. B* **82** 153204
[22] Sun F, Li N N, Chen B J and Jia Y T, Zhang L J, Li W M, Zhao G Q, Xing L Y, Fabbris G, Wang Y G, Deng Z, Uemura Y J, Mao H K, Haskel D, Yang W G and Jin C Q 2016 *Phys. Rev. B* **93** 224403
[23] Sun F, Zhao G Q, Escanhoela C A, Chen B J, Kou R H, Wang Y G, Xiao Y M, Chow P, Mao H K, Haskel D, Yang W G and Jin C Q 2017 *Phys. Rev. B* **95** 094412
[24] Peng Y, Yu S, Zhao G Q, Li W M, Zhao J F, Cao L P, Wang X C, Liu Q Q, Zhang S J, Yu R Z, Deng Z, Zhu X H and Jin C Q 2019 *Chin. Phys. B* **28** 057501
[25] Fu L C, Gu Y L, Zhi G X, Zhang H J, Zhang R F, Dong J O, Zhao X Q, Xie L F and Ning F L 2021 *Sci. Rep.* **11** 7652
[26] Zhang R F, Xu C C, Fu L C, Gu Y L, Zhi G X, Dong J O, Zhao X Q, Xie L F, Zhang H J, Cao C and Ning F L 2022 *J. Magn. Magn. Mater.* **554** 169276
[27] Rotter M and Tegel M and Johrendt D 2008 *Phys. Rev. Lett.* **101** 107006
[28] Singh Y, Green M A, Huang Q, Kreyssig A, McQueeney R J, Johnston D C and Goldman A I 2009 *Phys. Rev. B* **80** 100403
[29] Toby B H and Von Dreele R B 2013 *J. Appl. Crystallogr* **46** 544
[30] Glasbrenner J K, Žutić I and Mazin I I 2014 *Phys. Rev. B* **90** 140403
[31] Mulder C A M, van Duyneveldt A J and Mydosh J A 1981 *Phys. Rev. B* **23** 1384
[32] Lekshmi P N, Raji G R, Vasundhara M, Varma M R, Pillai S S and Valant M 2013 *J. Mater. Chem. C* **1** 6565